

SUPPORTING INFORMATION

Global Functional Connectivity Reorganization Reflects Cognitive Processing Speed Deficits and Fatigue in Multiple Sclerosis

Pavel Hok^{*,1,2,3}, Quang Thong Thai², Barbora Reháková^{4,5}, Martin Domin², Kamila Řasová⁶, Jaroslav Tintěra⁷, Martin Lotze², Matthias Grothe^{†,1}, Jaroslav Hlinka^{†,4}

¹*Department of Neurology, University Medicine Greifswald, Greifswald, Germany;*

²*Functional Imaging Unit, Institute of Diagnostic Radiology and Neuroradiology, University Medicine Greifswald, Greifswald, Germany;*

³*Department of Neurology, Faculty of Medicine and Dentistry, Palacký University Olomouc, Czechia;*

⁴*Department of Complex Systems, Institute of Computer Science of the Czech Academy of Sciences, Prague, Czechia;*

⁵*Department of Cognitive Neuroscience, Radboud University Medical Centre, Nijmegen, the Netherlands;*

⁶*Department of Rehabilitation, Third Faculty of Medicine, Charles University, Prague, Czechia;*

⁷*Radiodiagnostic and Interventional Radiology Department, Institute for Clinical and Experimental Medicine, Prague, Czechia.*

***) Corresponding Author**

MUDr. Pavel Hok, Ph.D.

Department of Neurology, University Medicine Greifswald

Ferdinand-Sauerbruch-Str. 1, 17475 Greifswald, Germany

Phone: +49 3834 86-6855

Fax: +49 3834 86-6875

Email: pavel.hok@med.uni-greifswald.de

URL: <https://www2.medizin.uni-greifswald.de/neurolog>

†) Both authors contributed equally to this work.

1. Supplementary Methods

1.1 Pre-processing

The initial pre-processing consisted of motion correction, correction of susceptibility-induced distortions and normalization to standard space using Advanced Normalization Tools (ANTs, v2.3.5.dev212-g44225).^{1,2} Brain coverage was evaluated using Mask_explorer.³ Next, motion outlier detection, anatomical component-based denoising procedure, and band-pass filtering within the frequency range 0.008 Hz – 0.09 Hz were applied in CONN toolbox v. 21a.⁴ Participants with maximum volume-to-volume displacement exceeding 2 mm and/or mean volume-to-volume displacement exceeding 2 standard deviations above the sample mean (i.e., >0.26 mm) were marked as outliers ($n = 13$). In the main analysis, all remaining steps were performed after excluding the outliers. However, additional sensitivity analysis consisting of the same steps was conducted in a parallel pipeline in the sample with outliers.

1.2 De-noising procedure

Segmentation of the T1-weighted structural image for the denoising procedure was carried out using CAT12 Toolbox (v.12.8r1932; Christian Gaser, Jena University Hospital), yielding gray matter, white matter and cerebro-spinal fluid masks in the MNI template space. Denoising was carried out using an anatomical component-based noise correction procedure (aCompCor),⁵ implemented in CONN toolbox v. 21a,⁴ incorporating linear regression of noise signal extracted from the subject-specific white matter and cerebrospinal fluid masks (5 time series from principal component analysis [PCA] of each source), a regressor for each outlier volume with excessive motion (criteria: composite motion > 0.9 mm or global signal volume-to-volume change beyond 5 standard deviations [SD]), and 6 motion parameters including their 6 first-order temporal derivatives (imported from previous preprocessing steps).

1.3 Voxel-wise whole-brain regions of interest (ROI)

A whole-brain voxel-wise parcellation consisted of 6-mm cubic regions of interest (ROIs) within the group-wise gray matter mask.⁶ To obtain the voxel-wise parcellation with approximately 6,000 ROIs, individual gray matter segments from T1-weighted images were averaged, down-sampled to a 6-mm space with trilinear interpolation, thresholded at $p < 0.3$, and binarized. The parcellation was finally masked with a down-sampled common brain mask based on blood oxygenation level-dependent (BOLD) data, yielding 4,632 ROIs.

1.4 Calculation of global degree rank order disruption index (k_D)

The k_D was calculated using custom Matlab script (available at https://github.com/pavelhok/calculate_kd/tree/MS-project) implementing a modified approach according to Achard et al.⁷ and Mansour et al.⁶ To overcome the necessity for an off-site control group as in Mansour et al.,⁶ we employed random sampling of a half of the control group. First, mean nodal degree (see article Section 2.5 Data pre-processing and analysis in the main manuscript body for details on degree calculation) of the control group was subtracted from the degree of the corresponding node in each participant. The difference between individual nodal degree and the control group mean was then plotted against the control group mean and k_D was obtained using a linear regression ($y = k_D * x + b$), where y = individual nodal degree – mean control group nodal degree, x = mean control group nodal degree, and b = intercept of the regression. The procedure was repeated across 100 random splittings of the control group and final k_D in each patient and healthy control (HC) was calculated by averaging the k_D values obtained in each iteration. For each HC participant, the final averaged k_D was based on 100 splittings in which the participant was not included in the control group mean.

1.5 Post-hoc Analyses

In order to visualize local contributions to significant global correlations between k_D and clinical scores, a post-hoc voxel-wise analysis was performed in randomise, part of FSL v. 6.0.3.⁸ First, nodal

degree centrality was back-projected to the original 6-mm voxels. Next, general linear model with two-sample t-test (group differences) and regression contrast was employed to evaluate the correlation using non-parametric threshold-free cluster enhancement (TFCE) correction for multiple comparisons with 10,000 permutations and family-wise error corrected alpha = 0.05.

In case of significant correlations with Expanded Disability Status Scale (EDSS), Fatigue Scale for Motor and Cognitive Functions (FSMC) score, or Timed Up and Go Test (TUG), correlation with regional degree in the 18 pre-defined ROIs was additionally assessed using Spearman rank correlation to allow further interpretation.

1.6 Power Analysis

No k_D data in patients with multiple sclerosis (PwMS) for a power analysis were available. Based on a published difference in k_D between patients and HC of $|k_D| = 0.21$ in a different patient cohort,⁶ analysis results in a minimum sample of 12 participants to achieve power to detect a significant correlation of 90%. With the existing data set ($n = 64$) differences of down to $|k_D| = 0.09$ can be identified with the same power of 90%.

1.7 Figure preparation

Fig. 1 was created using an open-source Python implementation of Raincloud Plots available at <https://github.com/pog87/PtitPrince>. Fig. 2 was generated using SPSS v29.0.1.1 (IBM, Armonk, NY, USA). Plots for Fig. 3 and Fig. S4 were created in Matlab v. R2018a. Brain reconstructions and slices for Fig. 4 and Fig. S3 were prepared in Mango v. 4.1 1531 (<https://rui.uthscsa.edu/mango/>). Brain slices for Fig. S1 were prepared using FSLeyes v. 1.10.2 (FMRIB Centre, Oxford, UK, <https://fsl.fmrib.ox.ac.uk/fsl/fslwiki/FSLeyes>).

2. Supplementary Results

2.1 Study sample

Here, results including motion outliers (i.e., including 7 PwMS and 6 HCs with excessive motion levels were identified) are reported, whereas results without outliers (“final” sample) are provided in the main manuscript body. In the sample with outliers, median age in PwMS was slightly higher than in HCs (Table S6).

2.2 Group differences and group differentiation (hypotheses 1 and 2)

PwMS showed significantly lower degree rank order disruption index (k_D) compared to HCs (PwMS: median = -0.316, inter-quartile range [IQR] = 0.498; HCs: median = -0.082, IQR = 0.541; $p = 0.001$, Mann-Whitney U test).

For hypothesis 2a, the receiver operating characteristic (ROC) analysis for differentiation between PwMS and HCs yielded significant above-chance area under curve (AUC) for k_D (AUC = 0.667, $p = 0.001$, two-tailed asymptotic significance for null hypothesis AUC = 0.5), the left lateral parietal portion of the DMN (DMN-LLP; AUC = 0.677, $p < 0.001$), left hippocampus (AUC = 0.608, $p = 0.032$) and the ACC (AUC = 0.606; $p = 0.036$), see Table S7. In pair-wise comparisons, AUC for k_D was significantly higher than AUC for 11 ROIs and did not significantly differ from the remaining ROIs (Table S7).

For hypothesis 2b, we observed no significant improvement in a multiple logistic regression model differentiating between PwMS and HCs) after adding k_D as an additional regressor on top of gray matter volume (GMV), fractional anisotropy (FA), log(lesion load [LL]) (χ^2 step = 0.579, $p = 0.447$).

2.3 Correlation with cognitive processing speed (hypotheses 3 and 4)

We detected no significant correlation between k_D and Symbol Digit Modalities Test (SDMT; Spearman’s $\rho = 0.20$, $p = 0.111$, $n = 62$). In case of regional degree centrality (hypothesis 4a), no significant correlation was observed after correction for multiple comparisons, see Table S8. For hypothesis 4b, an ordinal regression model including GMV, FA, log(LL), age, gender, and years since

diagnoses as Symbol Digit Modalities Test (SDMT) score as regressors was not significantly improved after adding k_D (χ^2 step = 3.63, $p = 0.057$, likelihood ratio test, see Table S9).

2.4 Correlation with global disability, fatigue, and motor performance (exploratory hypotheses 5 and 6)

We detected a significant correlation between k_D and FSMC (Spearman's $\rho = -0.27$, $p = 0.030$, $n = 63$), but not for EDSS ($\rho = -0.08$, $p = 0.546$, $n = 63$) or TUG ($\rho = -0.16$, $p = 0.233$, $n = 58$). For hypothesis 6, k_D significantly improved an ordinal regression model including GMV, FA, log(LL), age, gender, and years since diagnoses as regressors of fatigue (FSMC), but not for EDSS or TUG (Table S9).

2.5 Relationship between k_D and structural imaging biomarkers (exploratory hypotheses 7 and 8)

We observed a significant correlation (hypothesis 7) between k_D and LL ($\rho = -0.27$, $p = 0.033$, $n = 63$), but no significant correlation with GMV ($\rho = 0.12$, $p = 0.354$, $n = 63$) or global FA ($\rho = 0.04$, $p = 0.731$, $n = 63$). All structural imaging parameters significantly differed between PwMS and HCs (hypothesis 8), see Table S10.

3. Supplementary Tables

Table S1. List of regions of interests (ROI)

Abbreviation	Description	Side	MNI coordinates (x, y, z) [mm] [†]	Size [voxels] [‡]	Source [§]
DMN-MPFC	default mode network, medial prefrontal cortex		1, 52, -3	34	
DMN-LP	default mode network, lateral parietal part	L	-40, -76, 32	32	CONN network atlas4 binary labels
		R	47, -66, 29	42	
DMN-PCC	default mode network, posterior cingulate cortex		1, -61, 37	161	
Put	putamen	L	-25, 0, 1	32	
		R	26, 2, 1	29	
Cau	caudate nucleus	L	-13, 10, 10	15	
		R	15, 11, 11	20	
GP [¶]	globus pallidus	L	-24, -6, -6	1	HOSA ⁹⁻¹² 25% maximum probability labels
		R	18, 6, 0	1	
Tha	thalamus	L	-8, -20, 7	37	
		R	11, -20, 8	38	
Hip	hippocampus	L	-27, -21, -15	21	
		R	28, -21, -14	24	
Crbl	cerebellum		2, -61, -31	461	MNI structural atlas ^{13,14} 25% maximum probability labels
SPL	superior parietal lobule	L	-18, -63, 57	18	
		R	21, -66, 51	17	
DLPFC	dorsolateral prefrontal cortex	L	-24, -3, 51	9	Spherical ROI (d = 18 mm) centered according to Grothe et al. ¹⁵
		R	33, 0, 60	13	
ACC	anterior cingulate cortex		9, 15, 39	9	

Notes: [†]Atlas ROIs: coordinates are centers of mass of final ROIs, spherical ROIs: coordinates are centers of original spheres; [‡]voxel size 6×6×6 mm; [§]All ROIs were additionally masked with common gray matter and functional brain mask; [¶]region excluded from analyses due to small size after resampling.

Abbreviations: HOSA – Harvard-Oxford subcortical atlas, L – left; MNI – Montreal Neurological Institute; R – right; ROI – region of interest.

Table S2. Summary of outcome measures, regressors and statistical tests

Number	Hypothesis	Outcome measures	Regressors	Confounders	Statistical Test
1	Group differences in k_D (primary outcome)	k_D	Presence of MS	none	Mann-Whitney U test
2	Differentiation between PwMS and HCs	Presence of MS	k_D regional degree from 18 ROIs	none	ROC analysis with AUC pairwise asymptotic comparisons
			k_D , GMV, FA, log(LL)	none	multiple logistic regression with likelihood ratio test [†]
3	Correlation with cognitive processing speed	SDMT	k_D	none	Spearman's rank correlation coefficient
4	Regression of cognitive processing speed	SDMT	regional degree from 18 ROIs	none	Spearman's rank correlation coefficient
			k_D , GMV, FA, log(LL)	age, sex, years since diagnosis	ordinal regression with likelihood ratio test [†]
Exploratory hypotheses					
5	Correlation with global disability, fatigue, and motor performance	FSMC, EDSS, TUG	k_D	none	Spearman's rank correlation coefficient
6	Regression of global disability, fatigue, and motor performance	FSMC, EDSS, TUG	k_D , GMV, FA, log(LL)	age, sex, years since diagnosis	ordinal regression with likelihood ratio test [†]
7	Relationship between k_D and structural imaging biomarkers	k_D	GMV, FA, log(LL)	none	Spearman's rank correlation coefficient
8	Group differences in structural imaging biomarkers	GMV, FA, log(LL)	Presence of MS	none	Mann-Whitney U test

Notes: [†]comparison of nested models with and without k_D .

Abbreviations: EDSS – Expanded Disability Status Scale; FA – fractional anisotropy; FSMC – Fatigue Scale for Motor and Cognitive Functions; GMV – gray matter volume; HCs – healthy controls; k_D – degree rank order disruption index; log(LL) – log(lesion load); MS – multiple sclerosis; PwMS – patients with MS; ROIs – regions of interest; SDMT – Symbol Digit Modalities Test; TUG – Timed Up and Go Test.

Table S3. Receiver operating characteristic (ROC) analysis for group membership – no outliers

ROI		AUC	p^{\dagger}	AUC difference [‡]	p^{\S}
DMN-MPFC		0.570	0.197	0.072	0.116
DMN-LP	L	0.671	0.001	-0.029	0.585
	R	0.572	0.188	0.070	0.222
DMN-PCC		0.510	0.860	0.132	0.128
Put	L	0.540	0.467	0.102	0.004
	R	0.547	0.384	0.095	0.008
Cau	L	0.573	0.182	0.069	0.034
	R	0.584	0.118	0.058	0.054
Tha	L	0.580	0.140	0.062	0.171
	R	0.571	0.191	0.071	0.139
Hip	L	0.560	0.267	0.082	0.075
	R	0.534	0.535	0.108	0.030
Crbl		0.526	0.628	0.115	<0.001
SPL	L	0.509	0.864	0.133	0.123
	R	0.502	0.966	0.140	0.030
DLPFC	L	0.506	0.917	0.136	0.059
	R	0.555	0.311	0.087	0.314
ACC		0.619	0.026	0.023	0.619

Notes: [†]Asymptotic one-tailed uncorrected p for null hypothesis: true area = 0.5, significant values at $p < 0.05$ marked in **bold**; [‡] $AUC_{kD} - AUC_{ROI}$; [§]Asymptotic two-tailed uncorrected p for null hypothesis: true area difference = 0, significant values at $p < 0.05$ marked in **bold**.

Abbreviations: ACC – anterior cingulate cortex; AUC – area under curve; Cau – caudate nucleus; Crbl – cerebellum; DLPFC – dorsolateral prefrontal cortex; DMN – default mode network: -LP – lateral parietal part, -MPFC – medial prefrontal cortex, -PCC – posterior cingulate cortex; Hip – hippocampus; L – left; Put – putamen; SPL – superior parietal lobule; Tha – thalamus; R – right; ROI – region of interest.

Table S4. Ordinal regression of clinical scores

Outcome measure	SDMT		EDSS		FSMC		TUG	
Model	No k_D	With k_D	No k_D	With k_D	No k_D	With k_D	No k_D	With k_D
Pseudo R² (Cox&Snell)	0.215	0.276	0.326	0.327	0.202	0.298	0.297	0.300
-2 Log Likelihood	375.129	370.642	252.124	252.077	374.630	367.449	387.036	386.810
χ^2	13.311	17.799	22.101	22.149	12.614	19.795	18.348	18.574
df	6	7	6	7	6	7	6	7
Model Sig.	0.038	0.013	0.001	0.002	0.050	0.006	0.005	0.010
k_D Wald	N/A	4.051	N/A	0.056	N/A	7.662	N/A	0.249
k_D Sig.	N/A	0.044	N/A	0.813	N/A	0.006	N/A	0.618
χ^2 step	4.49		0.05		7.18		0.23	
df	1		1		1		1	
p^\dagger	0.034		0.828		0.007		0.634	

Notes: [†]One-tailed likelihood ratio test.

Abbreviations: df – degrees of freedom; EDSS – Expanded Disability Status Scale; FSMC – Fatigue Scale for Motor and Cognitive Functions; k_D – degree rank order disruption index; n – number; N/A – not applicable; SDMT – Symbol Digit Modalities Test; TUG – Timed Up and Go Test.

Table S5. Group differences in structural imaging parameters – no outliers

	PwMS <i>n</i> = 56	HC <i>n</i> = 58	
	Median ±IQR	Median ±IQR	<i>p</i> [†]
Lesion load [mm³]	2682.7 ±4834.4	91.0 ±114.2	<0.001
log(Lesion load) [log(mm³)]	3.43 ±0.81	1.96 ±0.52	
Gray matter volume [cm³]	1410.3 ±236.4	1591.6 ±195.0	<0.001
Global FA	0.588 ±0.033	0.612 ±0.029	<0.001

Notes: [†]Mann-Whitney U Test.

Abbreviations: FA – fractional anisotropy; HC – healthy controls; IQR – interquartile range; PwMS – patients with MS.

Table S6. Demographic and clinical data – sample with and without outliers

	Enrolled subjects	Included subjects	
		With outliers	Final sample
HC			
Number	65	64	58
Gender [women/men]	32/33	31/33	27/31
Median age \pm IQR [yrs]	40.9 \pm 17	40.8 \pm 17	40.5 \pm 17
PwMS			
Number	65	63	56
Gender [women/men]	39/26	38/25	35/21
p^\dagger	0.291	0.214	0.095
Median age \pm IQR [yrs]	45.3 \pm 17	45.4 \pm 17	45.1 \pm 17
p^\ddagger	0.048	0.039	0.090
Diagnosis [n, %]	RRMS	38, 58.5%	35, 62.5%
	SPMS	20, 30.8%	15, 26.8%
	PPMS	6, 9.2%	5, 8.9%
	no data	1, 1.5%	1, 1.8%
Time since diagnosis \pm SD [yrs]	12.8 \pm 6.8	12.7 \pm 6.9	12.6 \pm 6.2
EDSS \pm IQR	4.5 \pm 2.3	4.5 \pm 2.0	4.5 \pm 2.5
SDMT \pm IQR	45 \pm 31	45 \pm 31	45 \pm 29
FSMC \pm IQR	57 \pm 23	57 \pm 23	57 \pm 23
TUG \pm IQR [s]	11.2 \pm 11	10.8 \pm 9	10.3 \pm 9

Notes: [†]) Fisher's exact test between PwMS and HCs; [‡]) Mann-Whitney U test between PwMS and HCs.

Abbreviations: EDSS – Expanded Disability Status Scale; FSMC – Fatigue Scale for Motor and Cognitive Functions; HCs – healthy controls; IQR – interquartile range; MS – multiple sclerosis; n – number; N/A – not applicable; PPMS – primary progressive MS; PwMS – patients with MS; RRMS – relapsing-remitting MS; SD – standard deviation; SDMT – Symbol Digit Modalities Test; SPMS – secondary progressive MS; TUG – Timed Up and Go Test; yrs – years.

Table S7. Receiver operating characteristic (ROC) analysis for group membership – with outliers

ROI		AUC	p^{\dagger}	AUC difference [‡]	p^{\S}
DMN-MPFC		0.585	0.094	0.082	0.060
DMN-LP	L	0.677	<0.001	-0.010	0.835
	R	0.586	0.094	0.081	0.132
DMN-PCC		0.526	0.621	0.141	0.079
Put	L	0.558	0.257	0.109	0.001
	R	0.573	0.156	0.094	0.004
Cau	L	0.583	0.103	0.083	0.006
	R	0.587	0.089	0.080	0.005
Tha	L	0.581	0.115	0.086	0.041
	R	0.575	0.146	0.092	0.042
Hip	L	0.608	0.032	0.059	0.152
	R	0.576	0.139	0.091	0.045
Crbl		0.531	0.547	0.136	<0.001
SPL	L	0.512	0.814	0.155	0.008
	R	0.522	0.675	0.145	0.012
DLPFC	L	0.504	0.937	0.163	0.018
	R	0.572	0.162	0.095	0.230
ACC		0.606	0.036	0.061	0.168

Notes: [†]Asymptotic one-tailed uncorrected p for null hypothesis: true area = 0.5, significant values at $p < 0.05$ marked in **bold**; [‡] $AUC_{kD} - AUC_{ROI}$; [§]Asymptotic two-tailed uncorrected p for null hypothesis: true area difference = 0, significant values at $p < 0.05$ marked in **bold**.

Abbreviations: ACC – anterior cingulate cortex; AUC – area under curve; Cau – caudate nucleus; Crbl – cerebellum; DLPFC – dorsolateral prefrontal cortex; DMN – default mode network: -LP – lateral parietal part, -MPFC – medial prefrontal cortex, -PCC – posterior cingulate cortex; Hip – hippocampus; L – left; Put – putamen; SPL – superior parietal lobule; Tha – thalamus; R – right; ROI – region of interest.

Table S8. Correlation between regional degree and clinical scores – with outliers

ROI	SDMT <i>n</i> = 62		FSMC <i>n</i> = 63		
		<i>rho</i> [†]	<i>p</i> [†]	<i>rho</i> [†]	<i>p</i> [†]
DMN-MPFC		-0.354	<i>0.005</i>	0.200	0.116
DMN-LP	L	0.062	0.635	0.098	0.443
	R	-0.129	0.318	0.251	<i>0.047</i>
DMN-PCC		-0.169	0.189	0.152	0.233
Put	L	-0.200	0.119	0.326	<i>0.009</i>
	R	-0.114	0.376	0.254	<i>0.044</i>
Cau	L	-0.184	0.153	0.341	<i>0.006</i>
	R	-0.199	0.121	0.323	<i>0.010</i>
Tha	L	-0.149	0.247	0.240	0.058
	R	-0.191	0.137	0.229	0.071
Hip	L	-0.170	0.188	0.172	0.178
	R	-0.306	<i>0.016</i>	0.236	0.063
Crbl		-0.243	0.057	0.357	<i>0.004</i>
SPL	L	-0.112	0.384	-0.131	0.304
	R	-0.170	0.186	-0.041	0.748
DLPFC	L	-0.143	0.266	-0.157	0.220
	R	-0.111	0.388	0.068	0.595
ACC		-0.104	0.421	0.006	0.960

Notes: [†]Spearman's rank correlation coefficient *rho*, significant correlations at Bonferroni-Holm-corrected alpha = 0.0028 are marked in **bold** type, significant correlations at uncorrected alpha = 0.05 are marked in *italics*.

Abbreviations: ACC – anterior cingulate cortex; Cau – caudate nucleus; Crbl – cerebellum; DLPFC – dorsolateral prefrontal cortex; DMN – default mode network: -LP – lateral parietal part, -MPFC – medial prefrontal cortex, -PCC – posterior cingulate cortex; FSMC – Fatigue Scale for Motor and Cognitive Functions; Hip – hippocampus; L – left; n – number; Put – putamen; SPL – superior parietal lobule; Tha – thalamus; R – right; ROI – region of interest; SDMT – Symbol Digit Modalities Test.

Table S9. Ordinal regression of clinical scores – with outliers

Regressand	SDMT		EDSS		FSMC		TUG	
Model	No k_D	With k_D	No k_D	With k_D	No k_D	With k_D	No k_D	With k_D
Pseudo R² (Cox&Snell)	0.230	0.274	0.320	0.321	0.125	0.212	0.296	0.301
-2 Log Likelihood	433.806	430.179	282.218	282.123	439.047	432.515	442.300	441.883
χ^2	16.227	19.855	24.333	24.427	8.441	14.973	20.394	20.810
df	6	7	6	7	6	7	6	7
Model Sig.	0.013	0.006	<0.001	0.001	0.208	0.036	0.002	0.004
k_D Wald	N/A	3.307	N/A	0.111	N/A	6.637	N/A	0.454
k_D Sig.	N/A	0.069	N/A	0.739	N/A	0.010	N/A	0.500
χ^2 step	3.63		0.09		6.53		0.42	
df	1		1		1		1	
p^\dagger	0.057		0.759		0.011		0.519	

Notes: [†]One-tailed likelihood ratio test.

Abbreviations: df – degrees of freedom; EDSS – Expanded Disability Status Scale; FSMC – Fatigue Scale for Motor and Cognitive Functions; k_D – degree rank order disruption index; n – number; N/A – not applicable; SDMT – Symbol Digit Modalities Test; TUG – Timed Up and Go Test.

Table S10. Group differences in structural imaging parameters – with outliers

	PwMS <i>n</i> = 63	HC <i>n</i> = 64	
	Median ±IQR	Median ±IQR	<i>p</i> [†]
Lesion load [mm³]	2765.2 ±5115.6	93.7 ±134.9	<0.001
log(Lesion load) [log(mm³)]	3.44 ±0.83	1.97 ±0.58	
Gray matter volume [cm³]	1399.8 ±250.0	1561.3 ±193.5	<0.001
Global FA	0.588 ±0.039	0.610 ±0.028	<0.001

Notes: [†]Mann-Whitney U Test.

Abbreviations: FA – fractional anisotropy; HC – healthy controls; IQR – interquartile range; PwMS – patients with MS.

4. Supplementary Figures

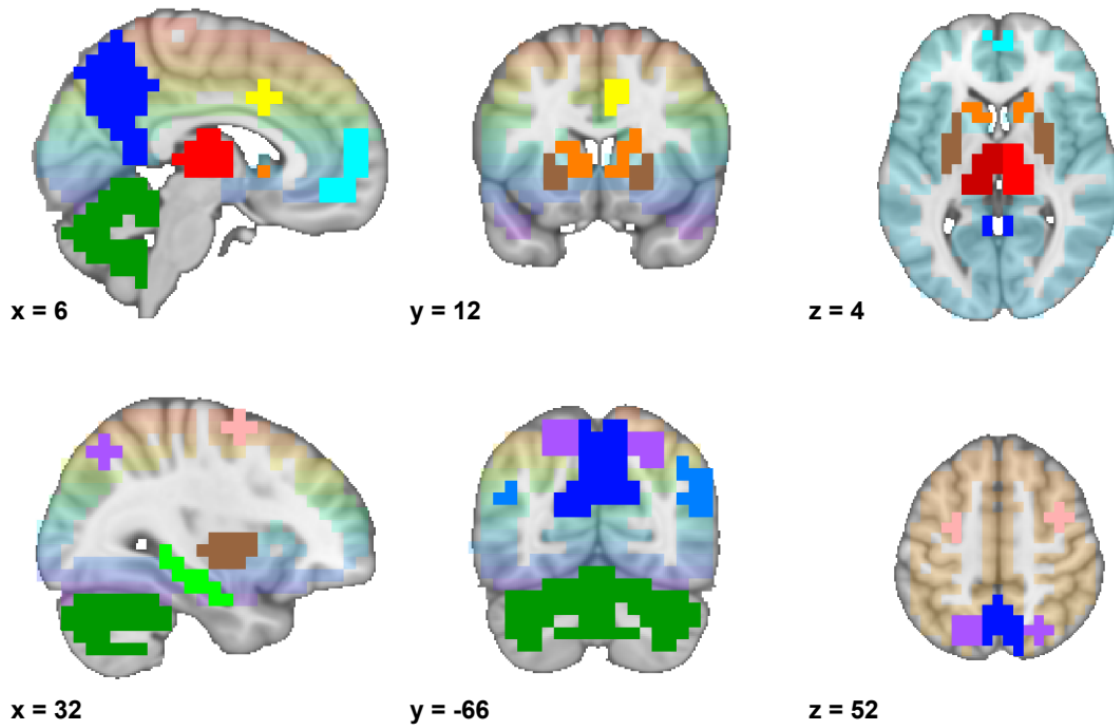


Fig. S1. Regions of interest (ROIs). Color overlays representing ROIs on top of orthogonal slices of the MNI152 standard brain template. Color coding: color spectrum (transparent background) – included 6-mm voxels; cyan - default mode network, medial prefrontal cortex; light blue - default mode network, lateral parietal cortex; dark blue – default mode network, posterior cingulate cortex; brown – putamen; orange – caudate nucleus; red (light & dark) – thalamus; light green – hippocampus; dark green – cerebellum; purple – superior parietal lobule; pink – dorsolateral prefrontal cortex; yellow – anterior cingulate cortex.

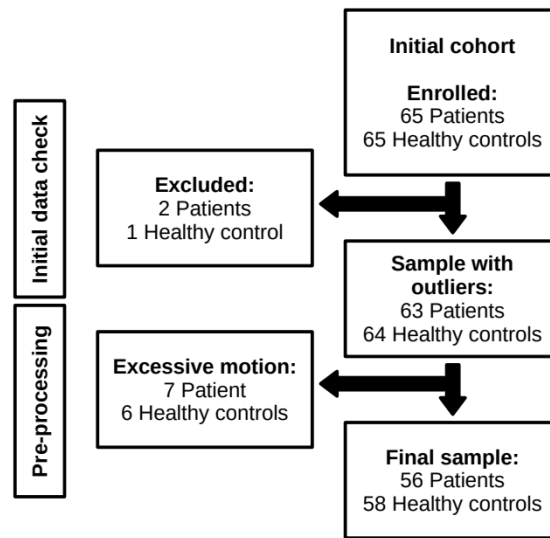


Fig. S2. Inclusion/exclusion diagram. Diagram illustrates exclusion rates at each step of the data analysis.

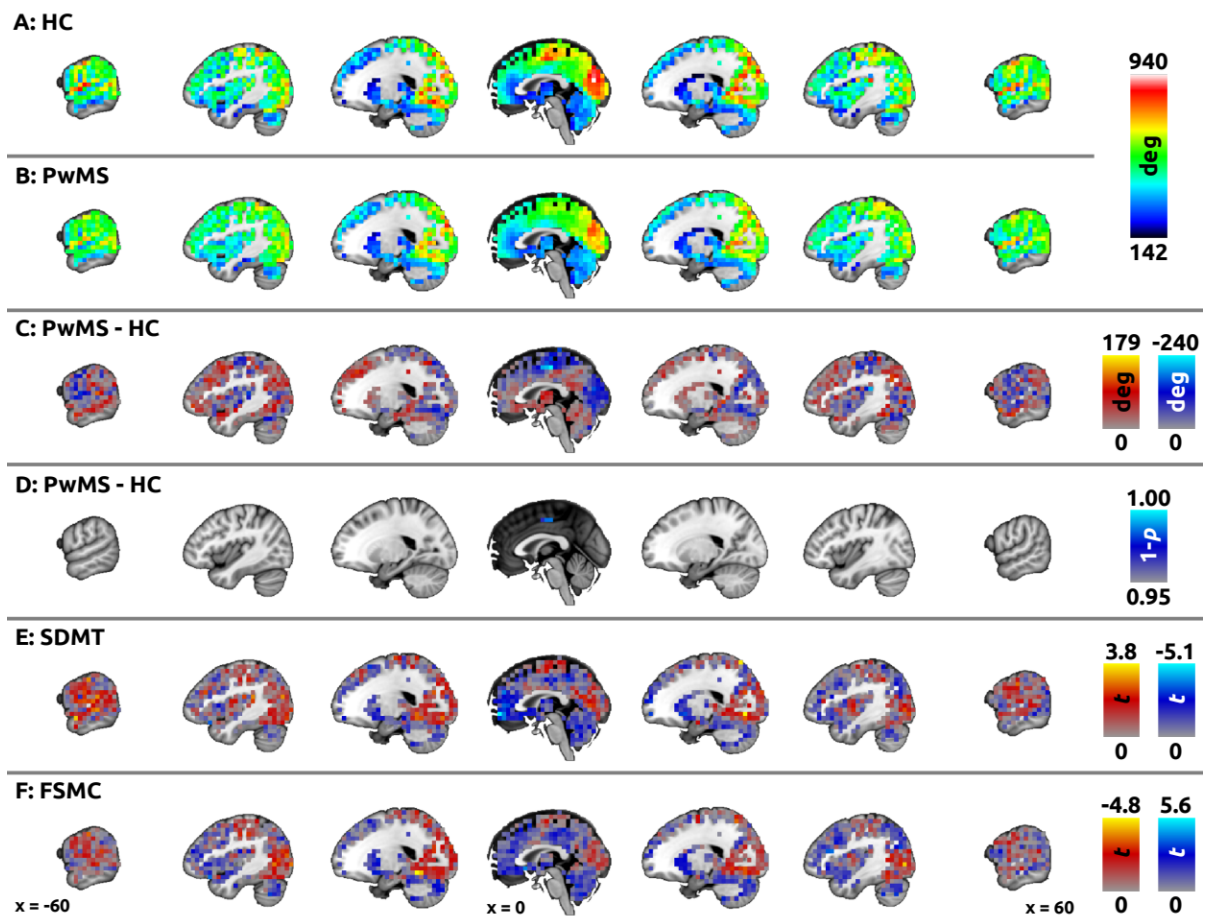


Fig. S3. Raw degree centrality, group degree differences, and unthresholded data. Color overlays on top of 1-mm MNI152 standard brain sagittal slices illustrate the underlying data for main analyses. In **panel A**, mean raw degree in healthy control (HC) group is shown (no outliers, $n = 58$). **Panel B** shows mean raw degree in patients with multiple sclerosis (PwMS, $n = 56$), using the same color scaling (actual range for PwMS = 172-843). **Panel C** shows mean difference individual degree in PwMS – mean normal degree in HC ($n = 56$), red overlay indicates higher degree in PwMS, blue overlay indicates higher degree in HC. In **panel D**, statistically significant group differences in raw degree are shown (thresholded using non-parametric threshold-free cluster enhancement with 10,000 permutations, family-wise error-corrected $p = 0.05$), with blue overlay indicating higher degree in HC in supplementary motor area and adjacent paracentral lobule. **Panels E-F** show unthresholded t-maps illustrating spatial distribution of linear regression of the degree centrality for (E) cognitive processing speed (Symbol Digit Modalities Test, SDMT) and (F) fatigue (Fatigue Scale for Motor and Cognitive Functions, FSMC). Here, color-coding was inverted for FSMC (positive correlation in blue, negative correlation in red) to match color coding for SDMT (in general, impairment is associated with lower SDMT, but higher FSMC).

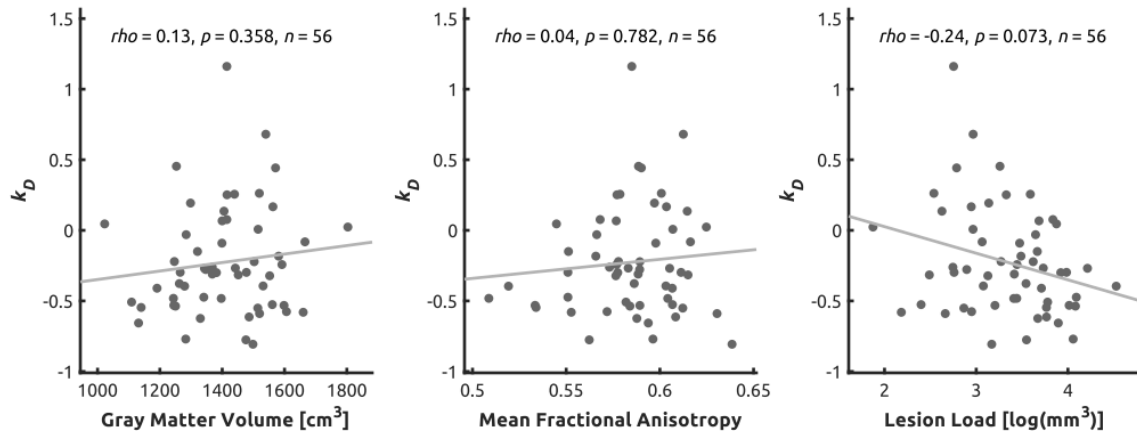


Fig. S4. Correlation between k_D and structural imaging. Scatter plots illustrating relationship between the degree rank order disruption index (k_D) and global gray matter volume, global white matter fractional anisotropy, and lesion load (after log transform). Spearman's rank correlation coefficient (ρ), two-tailed uncorrected significance, and number of valid observations are provided.

5. References

1. Avants BB, Tustison NJ, Song G, Cook PA, Klein A, Gee JC. A reproducible evaluation of ANTs similarity metric performance in brain image registration. *Neuroimage*. 2011;54(3):2033-2044. doi:10.1016/j.neuroimage.2010.09.025
2. Tustison NJ, Avants BB, Gee JC. Directly manipulated free-form deformation image registration. *IEEE Trans Image Process*. 2009;18(3):624-635. doi:10.1109/TIP.2008.2010072
3. Gajdoš M, Mikl M, Mareček R. Mask_explorer: A tool for exploring brain masks in fMRI group analysis. *Computer Methods and Programs in Biomedicine*. 2016;134:155-163. doi:10.1016/j.cmpb.2016.07.015
4. Whitfield-Gabrieli S, Nieto-Castanon A. Conn: A Functional Connectivity Toolbox for Correlated and Anticorrelated Brain Networks. *Brain Connectivity*. 2012;2(3):125-141. doi:10.1089/brain.2012.0073
5. Behzadi Y, Restom K, Liao J, Liu TT. A Component Based Noise Correction Method (CompCor) for BOLD and Perfusion Based fMRI. *Neuroimage*. 2007;37(1):90-101. doi:10.1016/j.neuroimage.2007.04.042
6. Mansour A, Baria AT, Tetreault P, et al. Global disruption of degree rank order: a hallmark of chronic pain. *Sci Rep*. 2016;6(1):34853. doi:10.1038/srep34853
7. Achard S, Delon-Martin C, Vértes PE, et al. Hubs of brain functional networks are radically reorganized in comatose patients. *Proc Natl Acad Sci U S A*. 2012;109(50):20608-20613. doi:10.1073/pnas.1208933109
8. Jenkinson M, Beckmann CF, Behrens TEJ, Woolrich MW, Smith SM. FSL. *Neuroimage*. 2012;62(2):782-790. doi:10.1016/j.neuroimage.2011.09.015
9. Makris N, Goldstein JM, Kennedy D, et al. Decreased volume of left and total anterior insular lobule in schizophrenia. *Schizophrenia Research*. 2006;83(2-3):155-171. doi:10.1016/j.schres.2005.11.020
10. Frazier JA, Chiu S, Breeze JL, et al. Structural Brain Magnetic Resonance Imaging of Limbic and Thalamic Volumes in Pediatric Bipolar Disorder. *Am J Psychiatry*. 2005;162(7):1256-1265. doi:10.1176/appi.ajp.162.7.1256
11. Desikan RS, Ségonne F, Fischl B, et al. An automated labeling system for subdividing the human cerebral cortex on MRI scans into gyral based regions of interest. *Neuroimage*. 2006;31(3):968-980. doi:10.1016/j.neuroimage.2006.01.021
12. Goldstein JM, Seidman LJ, Makris N, et al. Hypothalamic Abnormalities in Schizophrenia: Sex Effects and Genetic Vulnerability. *Biological Psychiatry*. 2007;61(8):935-945. doi:10.1016/j.biopsych.2006.06.027
13. Collins DL, Holmes CJ, Peters TM, Evans AC. Automatic 3-D model-based neuroanatomical segmentation. *Human Brain Mapping*. 1995;3(3):190-208. doi:10.1002/hbm.460030304

14. Mazziotta J, Toga A, Evans A, et al. A probabilistic atlas and reference system for the human brain: International Consortium for Brain Mapping (ICBM). *Philos Trans R Soc Lond B Biol Sci.* 2001;356(1412):1293-1322. doi:10.1098/rstb.2001.0915
15. Grothe M, Domin M, Hoffeld K, Nagels G, Lotze M. Functional representation of the symbol digit modalities test in relapsing remitting multiple sclerosis. *Mult Scler Relat Disord.* 2020;43:102159. doi:10.1016/j.msard.2020.102159